Supplement of The Cryosphere, 17, 4691–4704, 2023
https://doi.org/10.5194/tc-17-4691-2023-supplement

The Cryosphere
Open Access

Supplement of

Projection of snowfall extremes in the French Alps as a function of elevation and global warming level

Erwan Le Roux et al.

Correspondence to: Erwan Le Roux (erwan.le-roux@univ-grenoble-alpes.fr)

1 Supplementary Material Part A. General circulation models (GCMs) and regional climate models (RCMs)

RCMs	GCMs					
	CNRM-CM5	HadGEM2-ES	MPI-ESM-LR	EC-EARTH	IPSL-CM5A-MR	NorESM1-M
RCA4	✓	✓	✓	✓	✓	
CCLM4-8-17	✓	✓	✓	✓		
RACMO22E	✓		✓	✓		
ALADIN53	✓					
ALADIN63	✓					
REMO2009		✓				
RegCM4-6			✓			
WRF331F					✓	
WRF381P					✓	
HIRHAM5						✓
REMO2015						✓

Table 1. 20 GCM-RCM pairs considered. We always rely on the variant r1i1p1 except for EC-EARTH where we use r12i1p1.

2 Supplementary Material Part B. Quantile-quantile plots

A quantile-quantile (Q-Q) plot is a standard diagnosis tools based on the comparison of empirical quantiles (computed from the empirical distribution) and theoretical quantiles (computed from the expected distribution). For non-stationary GEV models, the approach is two-fold: i) we transform observations into residuals with a probability integral transformation, ii) we construct a Q-Q plot to assess if the residuals follow a standard Gumbel distribution. If this Q-Q plot reveals a good fit, it means that the non-stationary GEV model fits the data well (Coles, 2001; Katz, 2012; Le Roux et al., 2021).

In Figure 1, we display Q-Q plots of the selected model for the elevation 1500 m, which corresponds to the elevation illustrated in Figure 1. In this Figure, and in general, we observe that a majority of Q-Q plots show a good fit, as points stay close to the diagonal line. Yet, in general, we observe that empirical quantiles (for the residuals mentioned above) have a tendency to be larger than theoretical quantiles from the standard Gumbel distribution. In particular, for some selected models, the largest empirical quantile can largely overestimate the largest theoretical quantile (Fig. 1 **(d)**). This type of Q-Q plots, which might characterize a weak fit to the tail of the distribution, were found only at low elevations (Bauges massifs at 1200 m and 1500 m, Pelvoux massif at 1200 m and 1500 m, Chartreuse massif at 900 m, 1200 m and 1500 m, Maurienne massif at 900 m and 1200 m, Ubaye massif at 1500 m) and at high elevations (Chablais massif at 3000 m and 3300 m, Pelvoux massif at 3000 m, 3300 m and 3600 m, Thabor massif at 2700 m, 3000 m and 3300 m, Ubaye massif at 3300 m and 3600 m). This weak fit to the largest empirical quantile likely results from the typical high uncertainty in large quantiles.

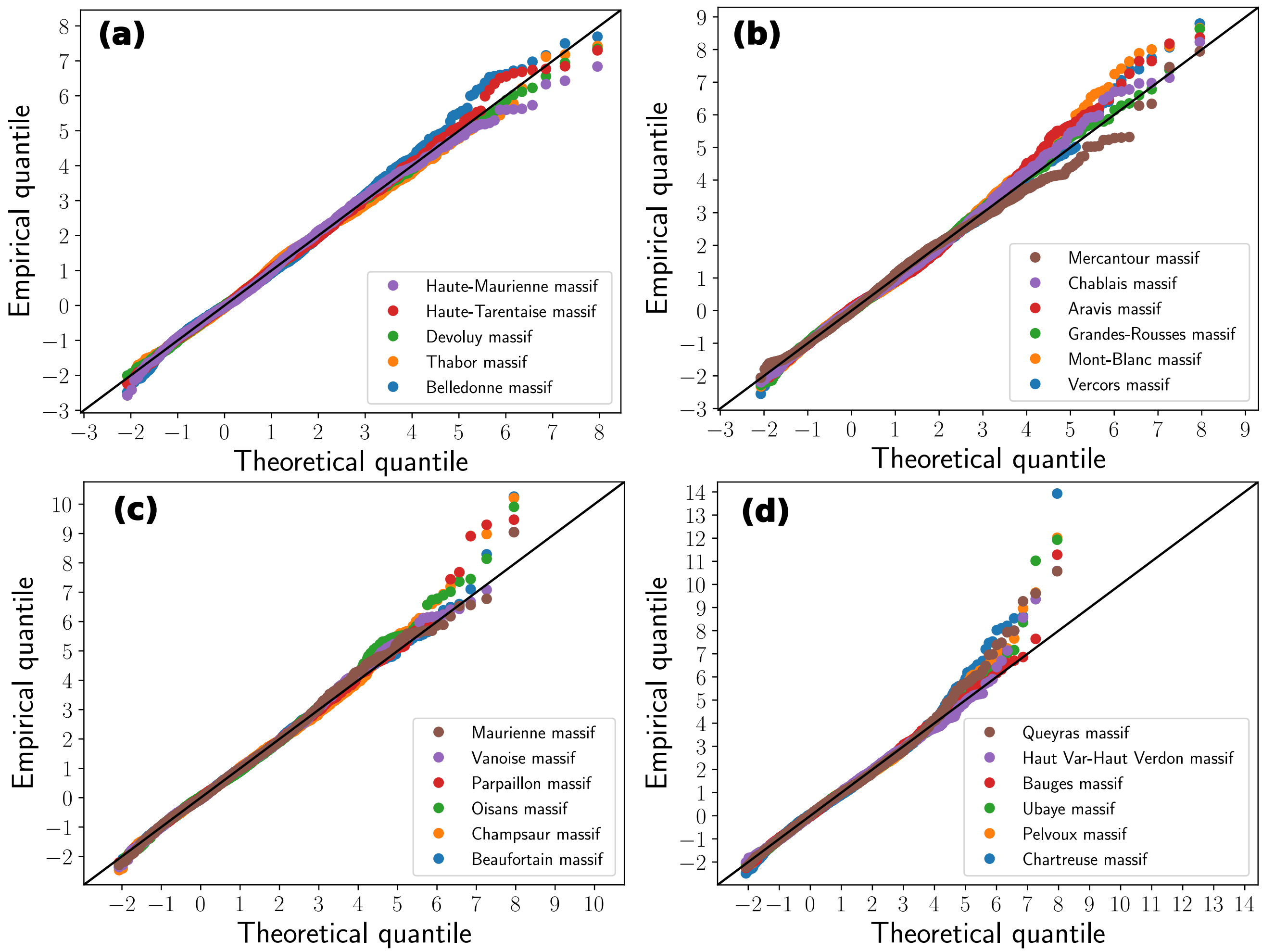

Figure 1. Q-Q plots of the selected models for daily maxima at the elevation 1500 m. **(a)** Best cases **(b, c)** Relatively good cases **(d)** Worst cases. These four type of cases **(a, b, c, d)** are sorted based on the value of the largest empirical quantile

3 Supplementary Material Part C. Analysis of the shape parameter values

On Figure 2, we illustrate the shape parameters of all selected models for daily snowfall. We have a total of 190 selected models, i.e. one model for each available massif and every 300 m of elevation from 900 m to 3600 m. We note that all shape parameters remain in a physically likely range, i.e. between -0.5 and 0.5 (Martins and Stedinger, 2000). Specifically, all shape parameters remain roughly between -0.10 and 0.17, expect one that increases steadily until reaching the value 0.4 at +4°C of global warming.

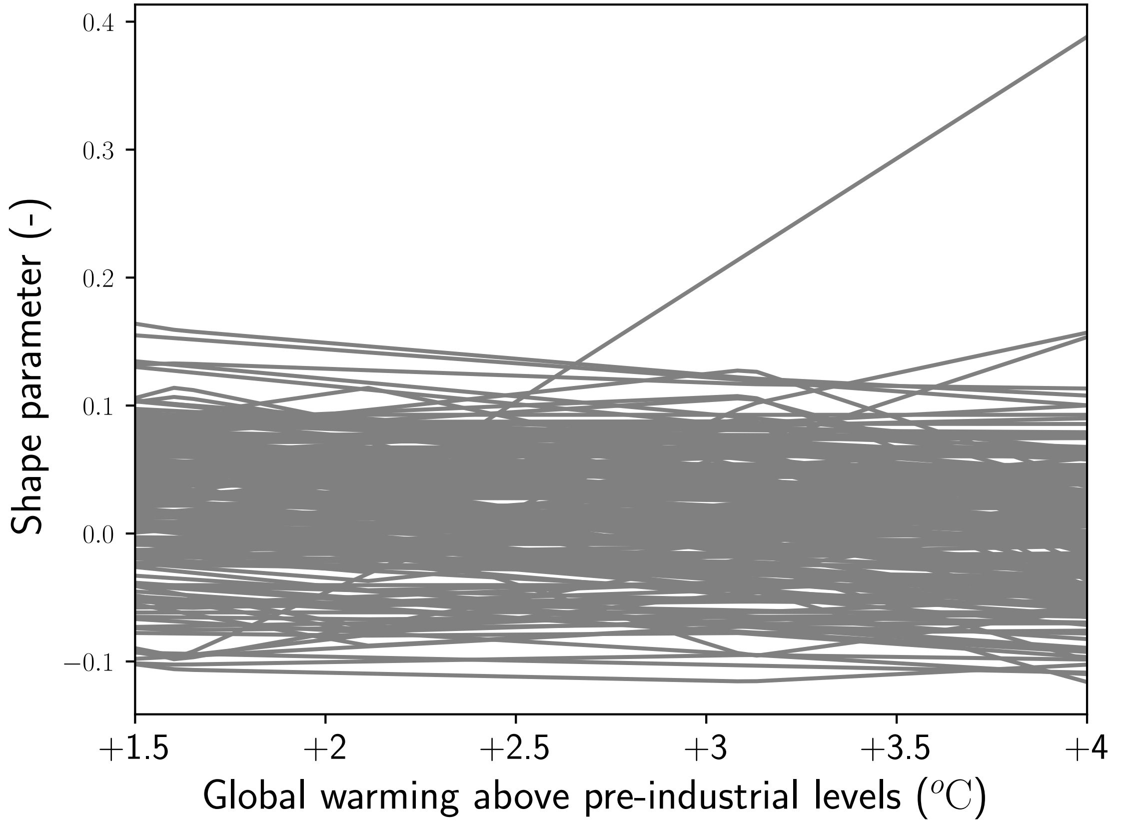

Figure 2. Shape parameter between +1.5 and +4°C of global warming of all selected models for daily snowfall.

4 Supplementary Material Part D. Projected changes in intense winter precipitation

In this appendix, we apply the methodology described in Section 3 to total (snow and rain) daily winter (December to February) precipitation. Figure 3 illustrates the average relative changes in heavy (mean annual maxima) and extreme (100-year return levels) winter precipitation between +1.5 and +4°C of global warming. We observe that both indicators are projected to increase for all elevations between 900 m and 3600 m. For a global warming of +4°C, average relative changes in 100-year return levels range between $+13\%$ and $+25\%$, while average relative changes in mean annual maxima range between $+4\%$ and $+14\%$

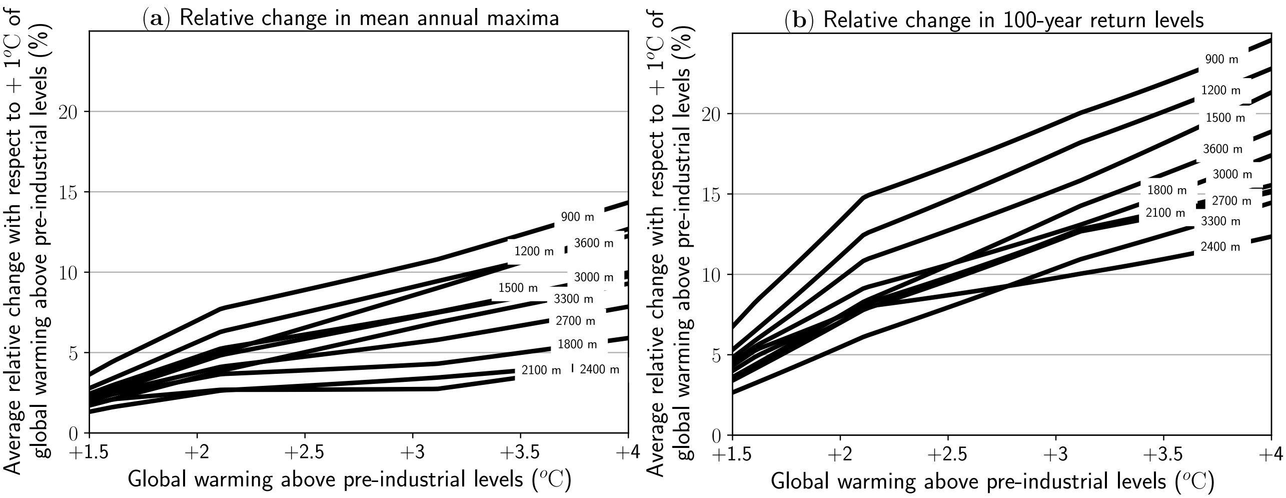

Figure 3. Average relative changes in **(a)** mean annual maxima **(b)** 100-year return levels of daily winter precipitation, every 300 m of elevation from 900 m to 3600 m, between +1.5°C and +4°C of global warming. Relative changes are computed with respect to +1°C.

5 Supplementary Material Part E. Projected changes in extreme snowfall accumulated over 3 days and 5 days

In this appendix, we apply the methodology described in Section 3 to maxima of snowfall accumulated over 3 days and over 5 days. Figure 4 illustrates the average relative changes in heavy (mean annual maxima) and extreme (100-year return levels) snowfall accumulated over 3 days between +1.5 and +4°C of global warming. On the other hand, Figure 5 illustrates the same result but for snowfall accumulated over 5 days. In general, relative changes trajectories observed for 3 days and 5 days are relatively comparable to the trajectories found for daily snowfall (Fig. 4). Differences are more clearly visible as global warming increases. On the one hand, at +4°C of global warming, relative decreases in mean annual maxima are projected to be more marked for snowfall accumulated over 3 days and 5 days compared to daily snowfall (note that Y-axis for Fig. 4 and Fig. 5 starts at -35%, while it starts at -30% for Fig. 4). For instance, relative changes in mean annual maxima at 900 m reach -26% for daily snowfall while it equals -31% and -32% for 3 days and 5 days, respectively. On the other hand, at +4°C of global warming, 100-year return levels are projected to have a larger relative increase for daily snowfall compared to snowfall in 3 and 5 days. For example, at 3600 m, the increase roughly equals +8% for daily snowfall while it equals +7% and +5% for snowfall accumulated over 3 days and 5 days.

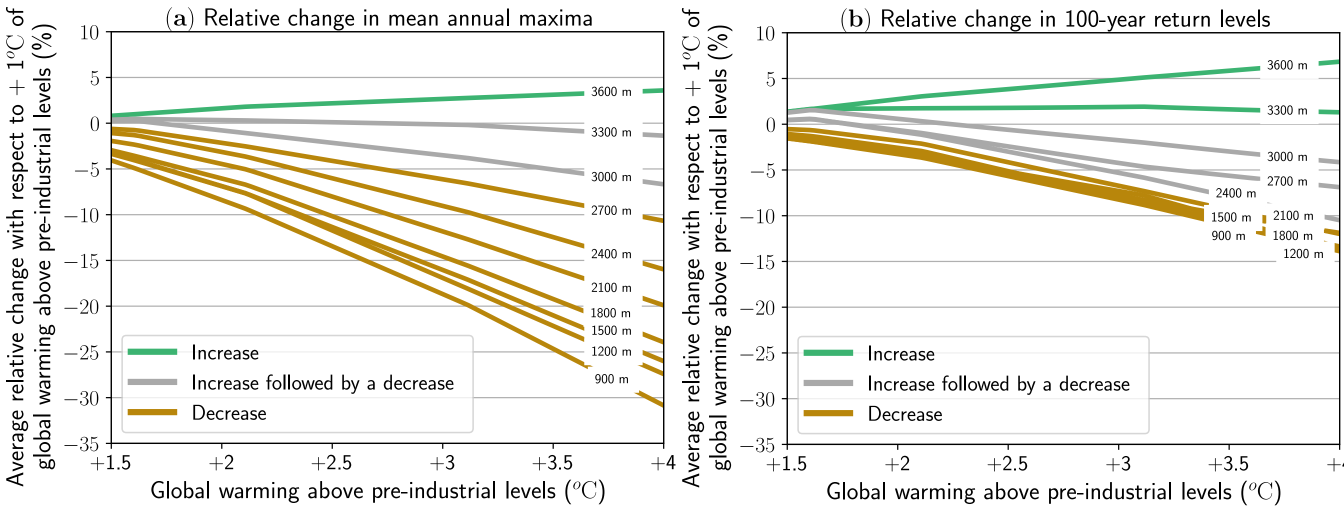

Figure 4. Average relative changes in **(a)** mean annual maxima **(b)** 100-year return levels of snowfall accumulated over 3 days, every 300 m of elevation from 900 m to 3600 m, between +1.5 and +4°C of global warming. Relative changes are computed with respect to the current climate (+1°C of global warming), and are averaged over all available massifs of the French Alps.

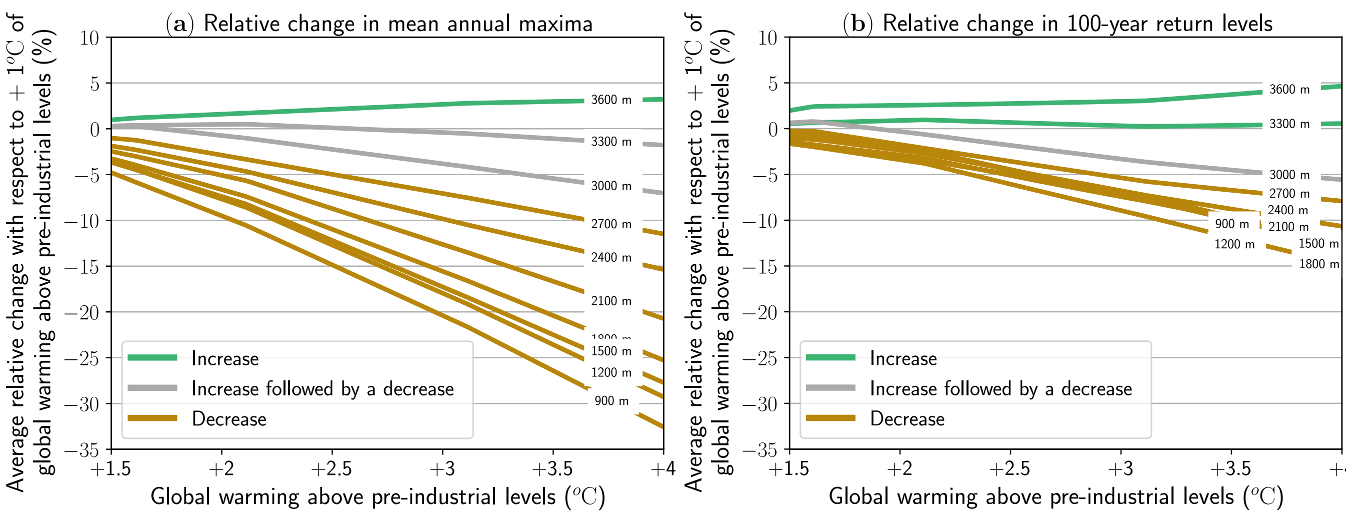

Figure 5. Average relative changes in **(a)** mean annual maxima **(b)** 100-year return levels of snowfall accumulated over 5 days, every 300 m of elevation from 900 m to 3600 m, between +1.5 and +4°C of global warming. Relative changes are computed with respect to the current climate (+1°C of global warming), and are averaged over all available massifs of the French Alps.

6 Supplementary Material Part F. Selected parametrization of the GEV distribution for daily snowfall

Table 2 indicates the selected parameterization of the GEV distribution for all massifs and all elevations from 900 m to 3600 m. We observe that 46% of these selected parameterizations consider one linear piece for the temporal non-stationarity of the GEV parameters. Simple linear trends are thus selected in most of the cases for the evolution of the GEV parameters. Similarly, the most parsimonious configuration is selected for 63% of the cases, i.e. without any adjustment coefficients. This means that adding a shift for the location or scale parameters of the GEV fitted to the projected annual maxima of daily snowfall with respect to the observed annual maxima does not usually improve the fitting of the GEV model. In other words, observed and projected annual maxima share the same parameterization for the majority of the fitted GEV models.

Parameterization of the adjustment coefficients	Number of linear pieces				Total
	1	2	3	4	
Zero	28%	11%	14%	11%	63%
One for all GCM-RCM pairs	0%	2%	1%	1%	3%
One for each GCM	4%	1%	2%	1%	8%
One for each RCM	6%	2%	1%	1%	9%
One for each GCM-RCM pair	9%	1%	3%	6%	18%
Total	46%	16%	20%	19%	100%

Table 2. Percentages of selected GEV parameterization (number of linear pieces for the temporal non-stationarity and adjustment coefficients) for all massifs and all elevations between 900 m and 3600 m.

References

Coles, S. G.: An introduction to Statistical Modeling of Extreme Values, vol. 208, Springer, London, https://doi.org/10.1007/978-1-4471-3675-0, 2001.

Katz, R. W.: Statistical methods for nonstationary extremes, in: Extremes in a Changing Climate - Detection, Analysis & Uncertainty, pp. 15–38, Springer Science & Business Media, https://doi.org/10.1007/978-94-007-4479-0, 2012.

Le Roux, E., Evin, G., Eckert, N., Blanchet, J., and Morin, S.: Elevation-dependent trends in extreme snowfall in the French Alps from 1959 to 2019, The Cryosphere, pp. 1–24, https://doi.org/10.5194/tc-2021-64, 2021.

Martins, E. S. and Stedinger, J. R.: Generalized maximum-likelihood generalized extreme-value quantile estimators for hydrologic data, Water Resources Research, 36, 737–744, https://doi.org/10.1029/1999WR900330, 2000.